Scanning Microscopy

Volume 1992
Number 6 *Signal and Image Processing in Microscopy and Microanalysis*

Article 12

1992

# Morphological Three-Dimensional Analysis

C. Gratin
*Ecole des Mines de Paris, France*, gratin@cmm.ensmp.fr

F. Meyer
*Ecole des Mines de Paris, France*

**Scanning Microscopy Supplement 6, 1992 (pages 129-135)** 0892-953X/92$5.00+.00
Scanning Microscopy International, Chicago (AMF O'Hare), IL 60666 USA

# MORPHOLOGICAL THREE-DIMENSIONAL ANALYSIS

C. Gratin* and F. Meyer

Centre de Morphologie Mathématique, Ecole des Mines de Paris,
35, Rue Saint Honoré, 77305 Fontainebleau Cedex, France

## Abstract

This paper presents the main results of our research on mathematical morphology for three-dimensional images. The first issue is to decide which grid must be used. The face-centred cubic grid and the centred cubic grid seem to be more suitable than the cubic grid in terms of possible rotations. For these two grids we derive the formulae for the basic Minkovski measures. Then we show through several examples that extension from 2D to 3D is straightforward for most transformations. The efficiency of direct 3D processing is illustrated by applications to filtering, overlapping particle separation and grey-scale image segmentation.

**Key Words**: Image segmentation, mathematical morphology, three-dimensional image analysis, three-dimensional grids, Minkowski measurements, non-linear filtering, distance function, watershed, foams, movement.

*Address for correspondence:
C. Gratin
Centre de Morphologie Mathématique,
Ecole des Mines de Paris,
35, Rue Saint Honoré,
77305 Fontainebleau Cedex,
France

Fax: 33 1 64 69 47 07
email: gratin@cmm.ensmp.fr

## Introduction

A variety of new technologies appeared in the last few years and is expanding rapidly with an increasing number of 3D images being produced in the fields of medical imaging, confocal microscopy, and more recently in electron microscopy. Besides the classical problem of visualization, there is a growing need to process these images in order to extract quantitative data. In other contexts, one has to filter images and extract some components of the 3D structure. For this reason we have extended the traditional methods of mathematical morphology to 3D images and have developed a 3D toolbox of methods able to cope with the main tasks in image processing.

We have found that the methods of mathematical morphology do not depend on the dimension of the space, and solutions are often found first in a one or two-dimensional space and then generalized to the three-dimensional case.

After a brief recall on grids and on the basic measures, we show a few examples of 3D transformations and explain how they can be combined to produce new operations like filters and segmentation tools. Their efficiency is illustrated through three applications:

1. filtering of noisy images,
2. separation of 3D overlapping particles in a polyurethane foam, and
3. segmentation of the left ventricle on a series of images of a human heart.

## Grids

For the construction of isotropic structuring elements, one desires the richest group of rotations possible. The choice of the grid also determines the connectivity relations of the figure, which are the basis of all geodesic transformations. The easiest solution, but also the poorest in terms of the group of rotations, is the cubic grid. The grid is obtained by piling up elementary cubes; the voxels being the vertices of the cube (Fig. 1-a). If one adds the centers of the cube, one gets the centred cubic grid (cc grid), also called body centred cubic grid (bcc grid) (Fig. 1-b & c). Alternatively one may add the centers of the faces of the cube and get the face-centred cubic grid (fcc grid) (Fig. 1-d). These last two grids gave richer neighborhood relations to each point, which is important for all geodesic transformations. They also gave a richer group of rotations of the grid; this will facilitate the design of isotropic transformations.

The design of the elementary 3D structuring elements easily follows from the choice of the grid: the rhombododecahedron for the cc grid which is a Steiner polyhedron (Fig. 2-a), and the cuboctahedron for the fcc grid which is not (Fig. 2-b).

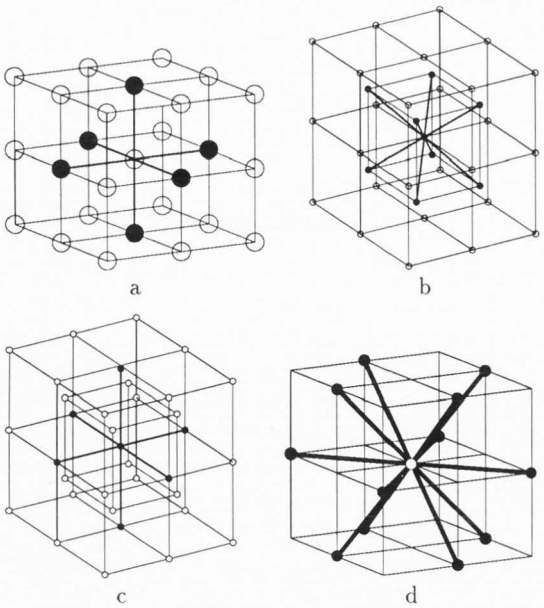


Figure 1: Grids and neigbourhoods in a 3D digital space: cubic (a), cc grid first (b) and second (c) neighbours, fcc grid (d).

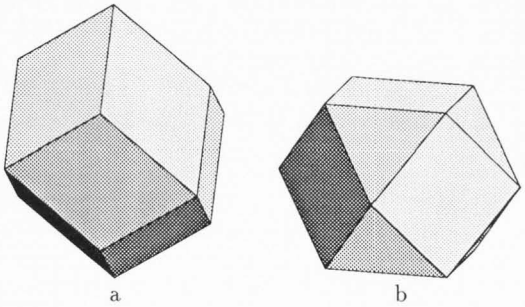


Figure 2: The cc's rhombododecahedron and the fcc's cuboctaedron.

## The Basic Minkovski Measurements in 3D

Mathematical morphology breaks down any image processing problem into a series of elementary image transformations. It turns out that the basic measurements are themselves an image transformation followed by a counting of voxels.

In the following, $\alpha$ stands for the length of the edge of the elementary cube in both cc and fcc grid. $v_0$ represents the volume of the influence zone of each point (the set of points closer to this point than to any other point).

**Binary images**

**The volume**. The estimation of the volume uses as test element a point. If $N$ is the number of vertices belonging to a set $V$, its volume is $N * v_0$.

**The surface**. The surface is given by the Crofton formula. For each direction $\beta$, one counts the number $N_\beta$ of intercepts. The surface of the projection of $X$ onto the plane perpendicular to $\beta$ is $S_\beta = N_\beta \times v_0/d_\beta$, where $d_\beta$ is the spacing between points on the line. The area is then:

$$S = 1/\pi \times \sum \omega_\beta \times S_\beta.$$

where $\omega_\beta$ is the solid angle associated with the direction $\beta$.

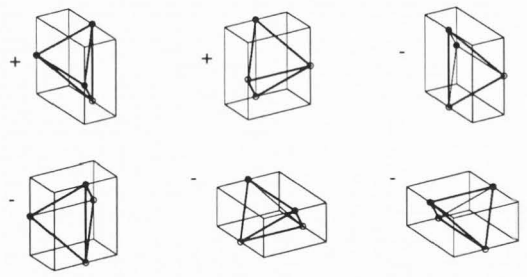


Figure 3: The 6 structuring elements necessary for estimating the Euler number in the cc grid.

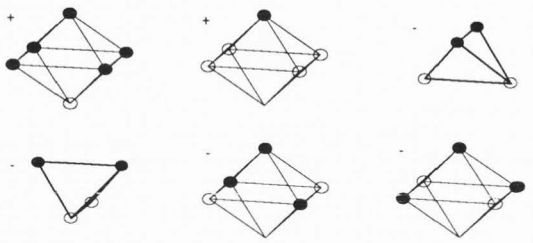


Figure 4: The 6 structuring elements necessary for estimating the Euler number in the fcc grid.

**The mean caliper diameter**. $D_\beta = N_\beta \times d_\beta$ where $N_\beta$ is the number of intercepts by test planes $P_\beta$, orthogonal to the direction $\beta$ and $d_\beta$ is the inter-plane distance.

$D$ = mean diameter for all directions $\beta$.

**The connectivity number**. The connectivity number is computed with the Euler formula:
$N = N(vertices) - N(edges) + N(faces) - N(volumes)$.
The computation of the Euler formula uses the smallest non decomposable volume elements of the grid, with which it is possible to fill space. In the cc grid, as well as in the fcc grid, the formula can be simplified so that only 6 terms remain. They are shown in Fig. 3 and Fig. 4.

More details about these results may be found in MEYER [9]. An analysis of the meaning of grey-tone measurements in 2D images may be found in SERRA [13].

**Grey-tone images**

**The volume**. The integral of the grey tones of all voxels within a 3D object gives the integrated density of this object. This may also be obtained by successive thresholds (i.e. the sum of the volumes of all thresholds within the 3D object).

**The surface**. The integral of the surfaces of all thresholds of a 3D grey-tone image is equal to the integral of the gradient of the image. This can be useful for characterizing 3D textures without any segmentation. One way to compute it is to measure the integral of the morphological gradient defined by $\delta(f) - \epsilon(f)$, where $\delta$ and $\epsilon$ stand for the dilation and the erosion respectively.

**The mean caliper diameter**. The integral of the mean caliper diameter for all thresholds gives a measure of the mean length of the grey-tone structures weighted by their grey level.

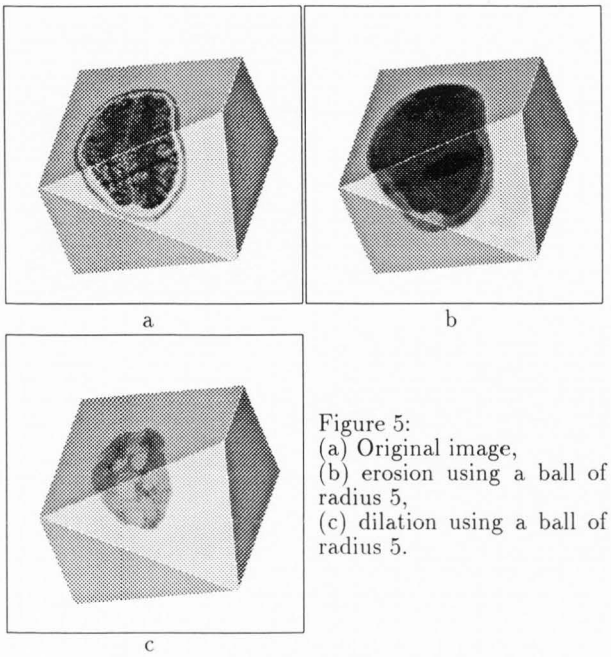

Figure 5:
(a) Original image,
(b) erosion using a ball of radius 5,
(c) dilation using a ball of radius 5.

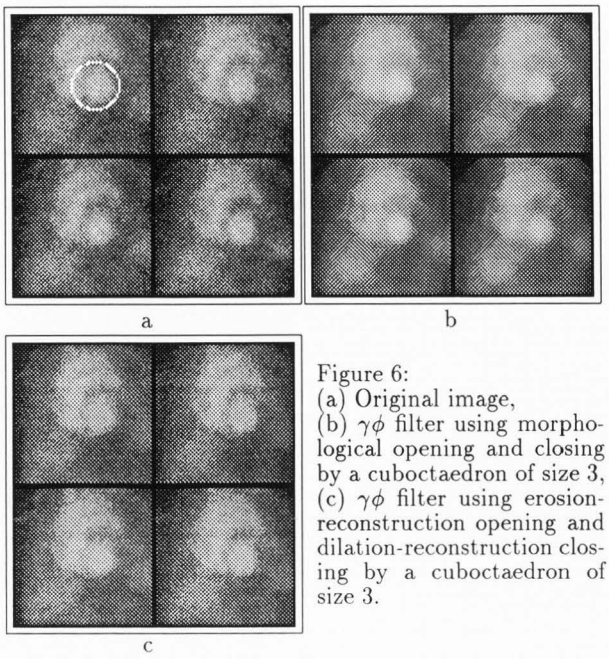

Figure 6:
(a) Original image,
(b) $\gamma\phi$ filter using morphological opening and closing by a cuboctaedron of size 3,
(c) $\gamma\phi$ filter using erosion-reconstruction opening and dilation-reconstruction closing by a cuboctaedron of size 3.

## Morphological Operations

### Erosions, dilations

Erosions and dilations are at the base of mathematical morphology. As soon as they are defined, almost all higher level transformations become accessible.

Their definitions are classical. Let $f$ be a 3D grey-tone function, $B$ a set of translations. We define the dilation of $f$ by $B$ by:

dilation: $\delta(f)(x) = Max_{t \in B} f(x+t)$
erosion: $\epsilon(f)(x) = Min_{t \in B} f(x+t)$

($x+t$ is the translated of voxel $x$).

Fig. 5 illustrates the results of 3D erosions and dilations on a magnetic resonance image of a brain.

### Openings, closings, application to filtering

Openings are defined as increasing, anti-extensive and idempotent transformations (SERRA [12]). An important class of them consist in erosions followed by dilations by the symmetric structuring element (morphological opening):

$$\gamma_B(f) = \delta_{\check{B}}(\epsilon_B(f)).$$

Symetrically, the morphological closing is defined by:

$$\phi_B(f) = \epsilon_{\check{B}}(\delta_B(f)).$$

Opening and closing act in a very antisymmetric way. The opening is anti-extensive ($\gamma(f) \leq f$) whereas the closing is extensive. In many situations, the information we want to suppress in an image is a mixture of white and dark particles. For such instances, a theory of morphological filters has been developed by MATHERON and SERRA in SERRA [13]: a morphological filter is defined as an increasing and idempotent transformation.

Let us present one precise example of such a filter applied to a noisy image: the $\gamma\phi$ filter (a closing followed by an opening). Fig. 6-a represents 4 images taken among a series of 30 heart images acquired during a beat cycle. The technique used produces low resolution and noisy images. We may consider the successive views of the beating heart as sections of a three-dimensional volume, where two dimensions are spatial and the third is time.

If we use the morphological opening and closing (Fig. 6-b) the result is not good: objects become connected and the contour of the left ventricle (circled in black in Fig. 6-a) is not preserved. But many other openings can be imagined. For instance we get better results if we use the opening (closing) obtained by an erosion (dilation) followed by a reconstruction (Fig. 6-c) (a presentation of geodesic transformations and in particular the grey-scale reconstruction may be found below).

For an easier understanding, we have shown the effect of the filter on binary images (Fig. 7). In the case of the heart, we have used grey-tone images. The result of the filtering may be appreciated best by comparing the gradient of the image before and after the filter (Fig. 8).

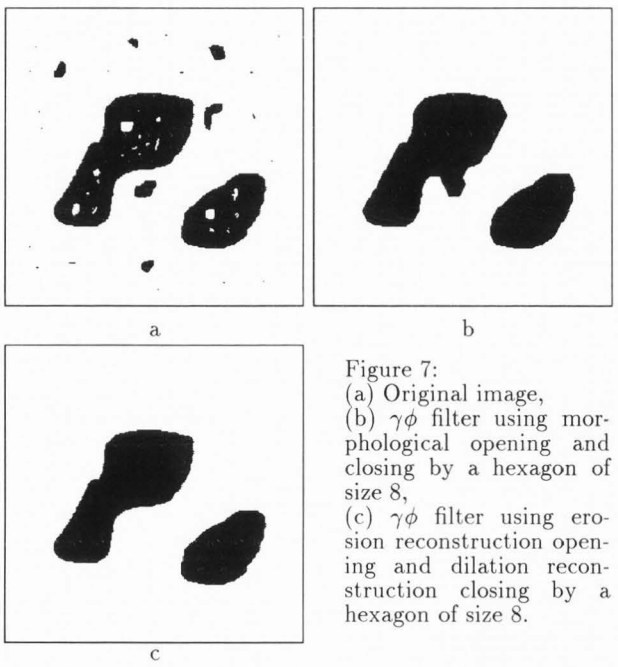

Figure 7:
(a) Original image,
(b) $\gamma\phi$ filter using morphological opening and closing by a hexagon of size 8,
(c) $\gamma\phi$ filter using erosion reconstruction opening and dilation reconstruction closing by a hexagon of size 8.

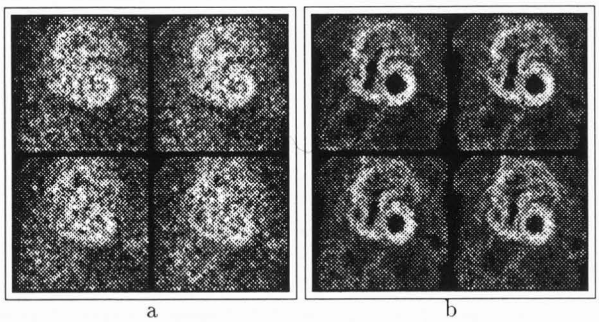

Figure 8: Gradient of the original image (a), and of the filtered image (b).

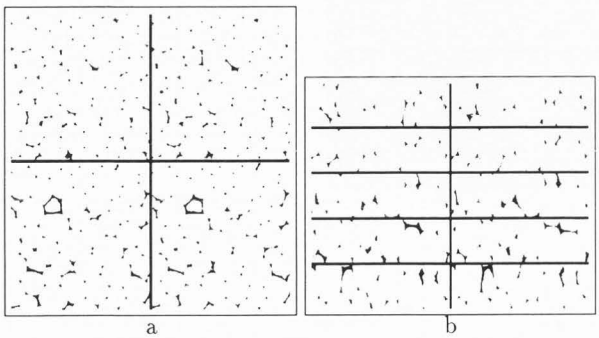

Figure 9: 4 (x,y) sections of a polyurethane foam (a), and 10 (x,z) sections (b).

**3D distance function and 3D watershed applied to the problem of separation of overlapping particles.**

Fig. 9 shows some of the 80 (x,y) sections of a polyurethane foam obtained by polishing. Our purpose is to extract the faces and edges of the elementary 3D cells in order to obtain a statistics on their size distribution. This will only be possible if we reconstruct entirely the 3D structure of the foam. Because of the very structure of the foam, the information contained in each section is only partial. However mathematical morphology provides an efficient methodology to individualize these cells, and this for either 2 or 3 dimensional images. It relies on the following three transformations: the distance function, the grey-scale reconstruction and the watershed transform.

**The distance function**:

The distance function of a binary set $X$ is a function $D(x)$ equal to the distance of $x$ to the background $X^c$:

$$\forall x \in X \quad D(x) = inf_{y \in X^c} d(x, y).$$

The distance $d(x, y)$ between two points $x$ and $y$ can be defined several ways. The most commonly used is the distance defined by the length of the shortest path joining $x$ to $y$, a path $(x_0, x_1, ..., x_N)$ being a sequence of points of the grid such that, for each $i$, $x_{i+1}$ is a neighbour of $x_i$. It is the easiest to compute, classically by means of a sequential algorithm (ROSENFELD [11], BORGEFORS [4]). If we want to get rid of the main directions of the grid one may use the euclidean distance as it is defined in the continuous space $IR^n$. But it is more difficult to obtain. DANIELSSON [5] proposes a sequential algorithm, SOILLE [14] gives an implementation using queues of pixels (or voxels) and GRATIN [7] uses hierarchical queues.

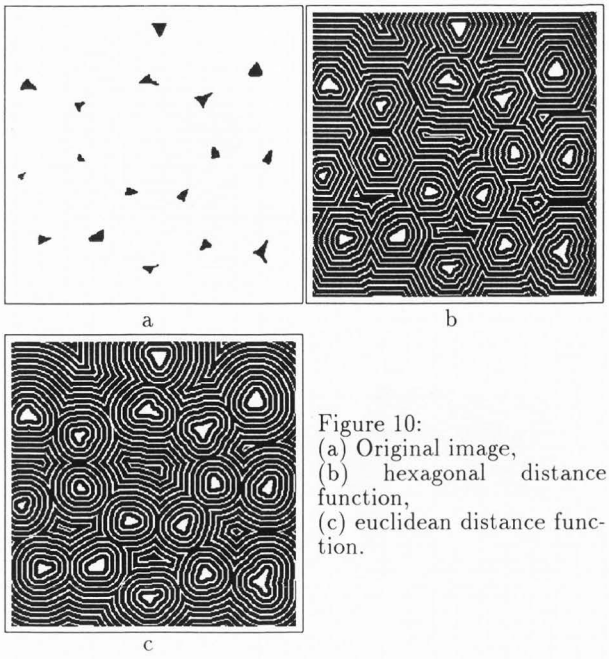


Figure 10:
(a) Original image,
(b) hexagonal distance function,
(c) euclidean distance function.

Figure 11: The grey-scale reconstruction.

Fig. 10 illustrates the distance function in the two dimensional case.

**The grey-scale reconstruction**:

Let $B$ be a flat structuring element, $f$ and $g$ be two functions such that $\forall x \quad g(x) \leq f(x)$.

The reconstruction of $g$ conditionally to $f$ is defined as $lim_{n \to +\infty} g_n$, where $g_0 = g$ and $g_n = inf(f, \delta_B(g_{n-1}))$.

Fig. 11 illustrates this operation in the one dimensional case.

One defines also the dual transformation: Let $f$ and $g$ be two functions such that $\forall x \quad g(x) \geq f(x)$.

The dual reconstruction of $g$ conditionally to $f$ is defined as $lim_{n \to +\infty} g_n$, where $g_0 = g$ and $g_n = sup(f, \epsilon_B(g_{n-1}))$.

As illustrated by Fig. 11, the main interest of the grey-scale reconstruction is the suppression of maxima. Whereas the function $f$ has three maxima, the reconstructed function has only two, generated by the maxima of the function $g$. In practice, we will often construct the function $g$ one of the following transformations of function $f$:

- $g = \epsilon(f)$ : erosion of $f$.
- $g = f - H$ : subtraction of a constant $H$ from $f$.

This last technique is used in Fig. 12: the distance function presents in some cells several maxima, whereas only one maximum is wanted. Subtracting a constant value $H$ and reconstructing the original function yields a new function with the desired feature: each cell has only one maximum in its centre.

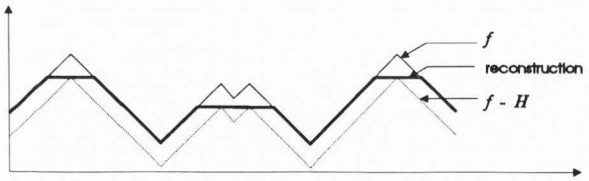


Figure 12: Filtering the distance function.

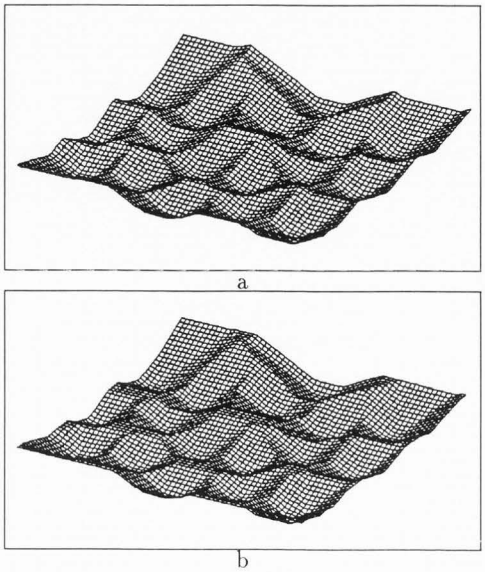


Figure 13: Original distance (a) and filtered distance with less maxima (b).

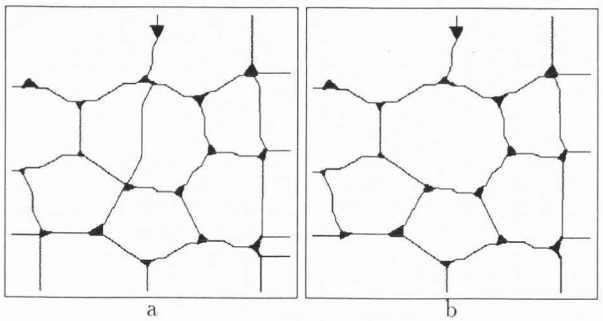


Figure 14: Separation obtained with the original euclidean distance (a) and with the filtered distance (b).

**The watershed line**:

The watershed line was introduced in image analysis by BEUCHER and LANTUEJOUL [3]. Since it has become the main tool for image segmentation, using mathematical morphology (MEYER, BEUCHER [10]). Although the watershed line is naturally a two-dimensional concept, its definition can easily be generalized to images of any dimension. An explanation may be found in BEUCHER [1,2].

**Application to the separation of overlapping particles**:

The common methodology is quite simple and is achieved in two steps:

1. computation of the distance function,

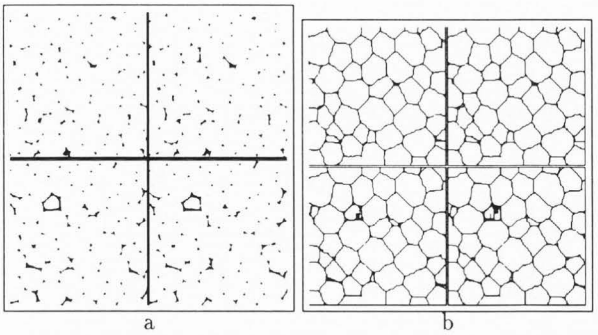


Figure 15: 4 (x,y) sections of the original image (a) and the result (b).

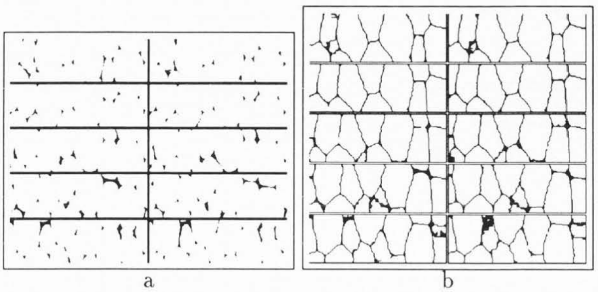


Figure 16: 8 (x,z) sections of the original image (a) and the result (b).

2. determination of the watershed line of the inverted distance function.

This algorithm segments the binary image into as many connected components as are present in the ultimate erosion, which are also the regional maxima of the distance function. Fig. 14-a shows that the result can be oversegmented. We can circumvent this problem by inserting between step 1 and 2 an additional step so as to filter the distance function. The technique that is usually used is the opening obtained by subtracting a constant value from the distance function. Then, the result is reconstructed conditionally to the original distance as illustrated in Fig. 12. GRATIN and MEYER [7] show that grey level grain reconstruction can be computed efficiently with the help of an algorithm based on hierarchical queues of pixels (voxels).

After this filtering step, the new function contains less maxima than the original one as can be seen in Fig. 13, so that the result is less oversegmented. In the ideal case, there remains only one maximum per particle. This ideal case is obtained in most situations.

Fig. 14-b shows the result of the watershed applied to the filtered distance.

The same methodology has been applied in 3D. The 3D euclidean distance was computed and filtered. The final result is shown Fig. 15 and Fig. 16 for some sections and compared to the original image. The entire image is presented in perspective in Fig. 17.

**Another example: segmentation of the left ventricle of the beating heart**

FRIEDLANDER [6] was the first to apply the 3D watershed transform on a series of images of the heart.

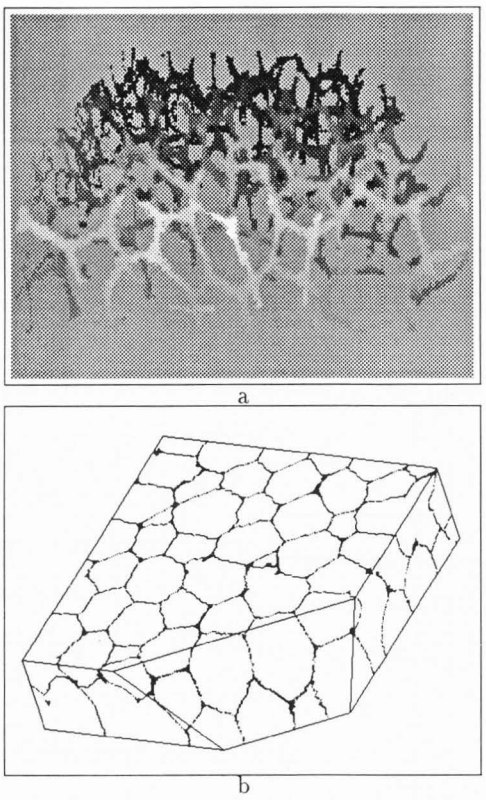

Figure 17: Views of the original image (a) and of the result (b).

GRATIN and MEYER [7] use it to extract the contour of a human brain in a real 3D image of magnetic resonance sections (the third dimension is a space dimension). The methodology was proposed by BEUCHER and MEYER in the late seventies, and is now widely used for segmentation problems, either 2D or 3D. It is called marker controlled segmentation. For a complete explanation, we refer again to BEUCHER [1,2].

FRIEDLANDER [6] uses as function a 3D laplacian of the original image, as inner markers one point in each image, placed inside the left ventricle, and as outer markers one rectangle in each image around and outside the left ventricle. Our approach is slightly different. In order to illustrate the efficiency of morphological filtering and segmentation tools we decided to use the smallest markers as possible. Thus we use as function the gradient (dilated - eroded) of the filtered image we obtained above, and as inner and outer markers two single points for the whole sequence, one placed inside and the other outside the left ventricle.

Fig. 18 shows the result obtained for 12 taken among the 30 images ($5^{th}$ to $16^{th}$). Inner and outer markers were placed both in the $15^{th}$ image. Of course the result could be improved by using more precise markers, but this example shows that good results can already be obtained even with small contextual information. This result can perfectly be used to determine good markers for an other step of segmentation. Note that SOILLE and VINCENT [15] and MEYER [8] gave two fast implementations of the watershed transform so that computing two watershed lines is no longer an expensive task in terms of processing time.

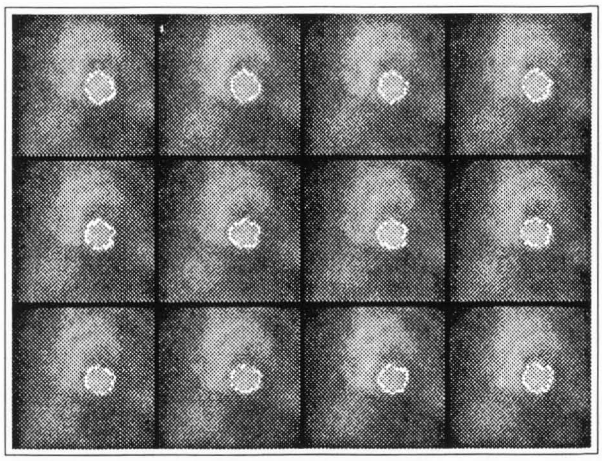

Figure 18: Result of the segmentation.

## Conclusion

True three-dimensional algorithms have proved to be better performing than solely the exploitation of two dimensional results. For example no matching of the contours found in the different sections is needed. Because there is no privileged direction, contours are build at the same time in the three dimensions of the space.

The 3D watershed transform and the marker controlled segmentation methodology provided a very simple and natural way to extract 3D objects, either true 3D or time sequences of 2D objects, either binary as seen for the polyurethane foam or grey-scale.

Finally, the wide availability of work stations, the increasing speed of processors and the appearance of optimal algorithms, make it now possible for these tools to come out of the laboratory into widespread use.

## Acknowledgements

The study on the polyurethane foam has been made under a contract with SHELL Research Belgium. The work has been done in collaboration with Mrs P. DELZENNE from the same company.

## References

[1] Beucher S. (1992). The watershed transformation applied to image segmentation. Scanning Microsc. Suppl. 6, 299-314.

[2] Beucher S. (1990). Segmentation d'Images et Morphologie Mathématique (Image Segmentation and Mathematical Morphology), PhD Thesis, School of Mines, Paris, France.

[3] Beucher S, Lantuéjoul C. (1979). Use of watersheds in contour detection. Proc. Int. Workshop on image processing, real-time edge and motion detection/estimation, CCETT, INSA, IRISA, Rennes, France, 2.1-2.12.

[4] Borgefors G. (1986). Distance transformations in digital space. Computer Vision, Graphics, and Image Processing, 34, 344-377.

[5] Danielsson PE. (1980). Euclidean distance mapping. Computer Graphics and Image Processing, 14, 227-248.

[6] Friedlander F. (1989). Le traitement morphologique d'images de cardiologie nucléaire (Morphological Processing of Nuclear Cardiology Images). PhD thesis, School of Mines, Paris, France.

[7] Gratin C, Meyer F. (1991). Mathematical morphology in three dimensions. Proc. of the $8^{th}$ Int. Conf. on Stereology, Irvine, Ca, 551-558.

[8] Meyer F. (1991). Un algorithme optimal de ligne de partage des eaux (An optimal algorithm for the computation of the watershed lines). Proc. $8^{th}$ Congres Reconnaissance des Formes et Intelligence Artificielle, AFCET, 847-857.

[9] Meyer F. (1992). Mathematical Morphology: from 2D to 3D. Journal of Microscopy, 164(1), 5-28.

[10] Meyer F, Beucher S. (1990). Morphological segmentation. Journal of visual Communication and Image Representation, 1(1), 21-46.

[11] Rosenfeld A. Pfaltz J.L. (1966). Sequential operations in digital picture processing. J. Assoc. Comp. Mach., 13, 471-494.

[12] Serra J. (1982). Image Analysis and Mathematical Morphology. Academic Press, London. Chapter 10.

[13] Serra J. (1988). Image Analysis and Mathematical Morphology, Vol. 2, Theoretical Advances. Academic Press, London. Chapters 6 & 7.

[14] Soille P. (1991). Spatial distributions from contour lines: an efficient methodology based on distance transformations. Journal of Visual Communication and Image Representation, 2(2), 138-150.

[15] Soille P, Vincent L. (1990). Determining watersheds in digital pictures via flooding simulations. SPIE Vol.1360 Visual Communications and Image Processing'90, 240-250.

### Discussion with Reviewers

**J.C. Russ:** The reason to use bcc, hcp or fcc voxel arrangements in 3D is of course to increase the uniformity of neighbor distances, corresponding to the use of hexagonal rather than square pixels in 2D. The bias introduced by square pixels is easily demonstrated. In 2D, this can be entirely overcome for a square grid by the use of the Euclidean distance map for erosions and dialtions, and this permits using the much more convenient square pixel array. The same is true in 3D, only more so. For one thing, acquisition of images from devices such as confocal microscopes is clearly facilitated by simple cubic voxel arrays. For a second thing, the difficulty of performing classical erosion and dilation by checking all of the neighbor points increases in proportion to the dimension using a technique such as Danielsson's. These distinctions become even more important in identifying 3D feature skeletons using a classical iterative erosion method, vs. constructing the medial axis transform from the distance map.

Authors: The reason to use BCC, hcp, or fcc voxel arrangements in 3D is not only to increase the uniformity of neighbor distances, goal which may be more easily achieved by using euclidean distance functions (despite the fact it demands a lower computational load to compute chamfer distances on a neighborhood). There are many other reasons to use a grid with the highest possible isotropy. Among them:

- the theory of measurement. The basic Minkowsky measurements compute the number of intercepts with test lines or test planes. The accuracy of measurements is connected to the number of directions taken into account.

- directional morphology. It is often necessary to analyze non isotropic phenomena. To do so, it is necessary to use linear transformations, which are much more easy to perform with a richer set of directions.

Reviewer: Having a 3D reconstruction of an object from a series of 2D images does often help to make (qualitative) conclusions related to the research being done. For quantitative purposes one must be sure that the 3D reconstruction is correct: that no artefacts were produced during image processing. I am interested if you could indicate in what way (if at all possible) one could verify whether the 3D reconstruction is an unbiased estimate of the "true" 3D object using the techniques you describe.

Authors: How to reach quantitative purposes in image processing is a difficult question, whose answer requires to consider the following aspects:

- digitalization: is the object correctly represented, without loss of details ? Do the transformations which are used allow a quantitative treatment ? These considerations are discussed in the book of J.Serra [12] in chapter I.B (the four principles of quantification), chapter V (Morphological parameters and set models), chapter VII (digitalization), and chapter VIII (Random Sampling).

- production of artefacts: it is impossible to discuss this problem in its generality. Let us focus on the segmentation of foam. The segmentation involves the following steps: (a) construction of the distance transform, (b) filtering of the distance function, and (c) construction of the watershed line of the inverted filtered distance function.

Several questions arise: risk of over or under segmentation of cells, fidelity of the walls which are generated.

Risk of over or under-segmentation: oversegmentation arises when a cell is split in two parts because the filtered distance function has several maxima within the cell. This may occur if the cells are very elongated with slightly fluctuating shapes. This will occur much more frequently with a euclidean distance transform than with a more crude distance transform simply based on the neighborhood graph. On the contrary, under-segmentation occurs if two particles are so intertwined that the distance function has only one maximum within them. But who will appreciate the significance of this over or under-segmentation ? In one case, metallography for example, the expert considers that over-segmentation has occurred, because the fluctuations of shape are not relevant. With the same images, a microbiologist may consider that the segmentation is correct, because the objects are dividing bacteria. That means that one has to tune the filtering of the distance function to the domain of application. Fidelity of the walls: if the cells are correctly marked, the watershed line constructs a separating wall between them. If one is interested simply in the measurement of the neighborhood relationships between cells, the shape of the wall is not important. If one is interested in the area or direction of the wall, the issue of wall fidelity is much more important. In this case, it becomes important to chose a euclidean distance function rather than a connective one.